Evaluation of mesoporous carbon aerogels as carriers of the non-steroidal anti-inflammatory drug ibuprofen

Accepted Manuscript

Title: Evaluation of mesoporous carbon aerogels as carriers of the non-steroidal anti-inflammatory drug ibuprofen

Author: Georgios K. Eleftheriadis Maria Filippousi Vassiliki Tsachouridou Maria-Anna Darda Lamprini Sygellou Ioanna Kontopoulou Nikolaos Bouropoulos Theodoros Steriotis Georgia Charalambopoulou Ioannis S. Vizirianakis Gustaaf Van Tendeloo Dimitrios G. Fatouros

PII: S0378-5173(16)30942-5
DOI: http://dx.doi.org/doi:10.1016/j.ijpharm.2016.10.008
Reference: IJP 16138

To appear in: *International Journal of Pharmaceutics*

Received date: 28-6-2016
Revised date: 1-10-2016
Accepted date: 4-10-2016

Please cite this article as: Eleftheriadis, Georgios K., Filippousi, Maria, Tsachouridou, Vassiliki, Darda, Maria-Anna, Sygellou, Lamprini, Kontopoulou, Ioanna, Bouropoulos, Nikolaos, Steriotis, Theodoros, Charalambopoulou, Georgia, Vizirianakis, Ioannis S., Van Tendeloo, Gustaaf, Fatouros, Dimitrios G., Evaluation of mesoporous carbon aerogels as carriers of the non-steroidal anti-inflammatory drug ibuprofen.International Journal of Pharmaceutics http://dx.doi.org/10.1016/j.ijpharm.2016.10.008

Evaluation of mesoporous carbon aerogels as carriers of the non-steroidal anti-inflammatory drug ibuprofen

Georgios K. Eleftheriadis,[1] Maria Filippousi,[2] Vassiliki Tsachouridou,[3] Maria-Anna Darda,[1] Lamprini Sygellou,[4] Ioanna Kontopoulou,[5] Nikolaos Bouropoulos,[5] Theodoros Steriotis,[6] Georgia Charalambopoulou,[6] Ioannis S. Vizirianakis,[3] Gustaaf Van Tendeloo,[2] Dimitrios G. Fatouros[1,*]

[1]School of Pharmacy, Department of Pharmaceutical Technology, Aristotle University of Thessaloniki, GR-54124

[2]EMAT, University of Antwerp, Groenenborgerlaan 171, B-2020 Antwerp, Belgium

[3]School of Pharmacy, Department of Pharmacology, Aristotle University of Thessaloniki, GR-54124

[4]Foundation for Research and Technology, Hellas-Institute of Chemical Engineering and High Temperature Chemical Processes (FORTH/ICE-HT), P.O. Box 1414, GR-26504 Patras, Greece

[5] Department of Materials Science, University of Patras, 26504 Rio, Patras, Greece

[6] National Center for Scientific Research "Demokritos", Agia Paraskevi Attikis 15341, Greece

*Corresponding author: Dr Dimitrios G. Fatouros,

e-mail: dfatouro@pharm.auth.gr

Tel: + 30 2310 997653

Fax: + 30 2310 997652

Graphical Abstract

Mesoporous carbon aerogels can modulate the release profiles of ibuprofen whereas in *vitro* toxicity profiles appear to be compatible as carriers for the oral delivery of poorly soluble drugs.

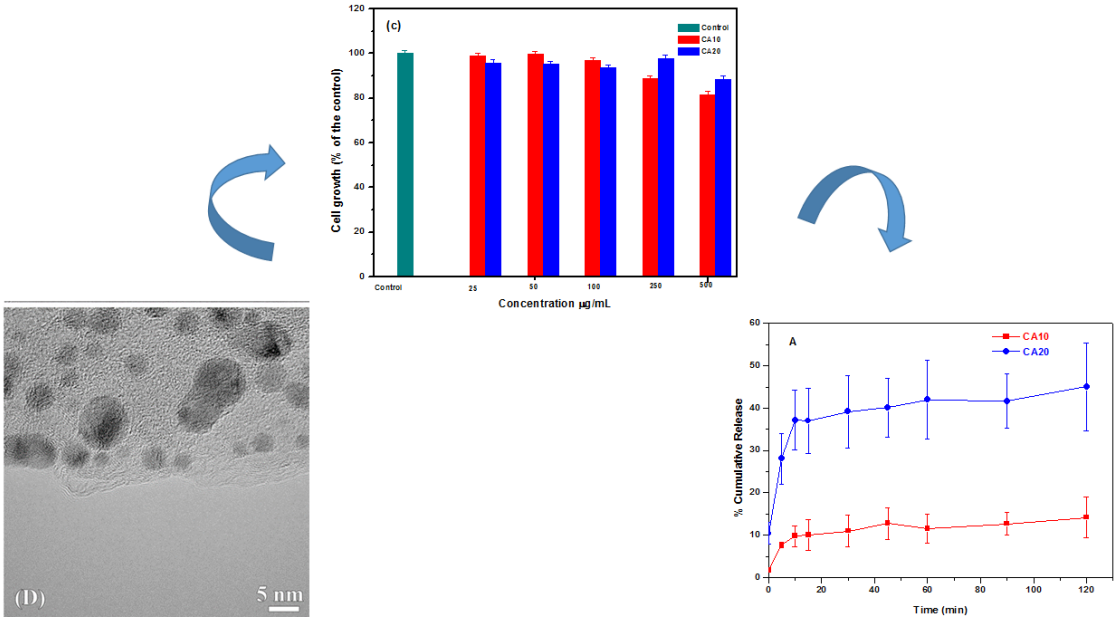

Abstract

Towards the development of novel drug carriers for oral delivery of poorly soluble drugs mesoporous aerogel carbons (CAs) namely CA10 and CA20 with different pore sizes (10 and 20 nm respectively) were evaluated. The non-steroidal anti-inflammatory lipophilic compound ibuprofen was incorporated *via* passive loading. The drug loaded carbon aerogels were systemically investigated by means of High-Resolution Transmission Electron Microscopy (HR-TEM), Nitrogen physisorption studies, X-ray diffraction (XRD), Differential Scanning Calorimetry (DSC), X-ray photon electron spectroscopy (XPS) and ζ-potential studies. *In vitro* release studies were performed in simulated intestinal fluids reflecting both fasted (FaSSIF) and fed (FeSSIF) state conditions. Cytotoxicity studies were conducted with human intestinal cells (Caco-2). Drug was in an amorphous state in the pores of the carbon carrier as

shown from the physicochemical characterization studies. The results showed marked differences in the release profiles for ibuprofen from the two aerogels in the media tested whereas *in vitro* toxicity profiles appear to be compatible with potential therapeutic applications at low concentrations.

Keywords: Carbon aerogels, poorly soluble drugs, simulated intestinal fluids, oral delivery

1. Introduction

The development of effective oral dosage forms for hydrophobic new chemical entities (NCE) continues to be a pressing issue for the pharmaceutical industry. Many of these poorly water-soluble NCE's readily permeate biological membranes, making their maximum solubility and/or dissolution rate in the gastro-intestinal tract (GIT) the rate-limiting steps to their absorption [Leuner and Dressman, 2000]. Among the different approaches to enhance drug dissolution mesoporous, [Santos et al. 2013; Vallet-Regi et al. 2001a; Vallet-Regi et al. 2007b, Salonen et al. 2005; Mellaerts et al. 2008] microporous materials [Fatouros et al. 2011; Spanakis et al 2014] and metal organic frameworks [Horcajada et al.; 2010; McKinlay et al. 2010] have been proposed as such agents.

In recent years mesoporous carbons have been emerged as a new class of mesoporous drug carriers due to their inertness, high specific high surface areas and nanosized pores [Karavasili et al. 2013; Zhao et al. 2014; Sanchez-Sanchez et al. 2015; Zhang et al. 2015a, Wan et al. 2015; Gao et al. 2015].

Carbon aerogels (CAs) comprise a special class of lightweight nanoporous materials with tuneable porosity and nanoarchitecture, typically derived from the calcination of CO2-supercritical-dried organic aerogels that are produced from sol-gel routes [Antonietti et al. 2014] (*e.g.* the polycondensation reaction of resorcinol with

formaldehyde) [Pekala et al. 1992]. The variation of the synthesis conditions (i.e., composition of the starting solution and temperature of the sol - gel process) allows tailoring of the particle and pore sizes in the range from a few nanometers (nm) up to some microns, whereas porosities up to 85 % can be achieved. CAs possess a tunable three-dimensional hierarchical structure and can be produced as thin films, powders, microspheres or monolithic materials. Their microstructure typically consists of interconnected nanometer-sized carbon particles (3 - 30 nm) with small interstitial pores (< 50 nm) and sharp pore size distributions, while the presence of microporosity due to the carbonization step is common.

To the best of our knowledge this is the first report investigating the potential of these materials as drug delivery carriers of poorly soluble drugs. For the present work two different CA samples with nominal mean pore size 10 and 20 nm (denoted hereafter as CA10 and CA20) were evaluated for their loading capacity of a poorly soluble compound namely; ibuprofen (IBU), and characterized by an array of physicochemical methods. *In vitro* release studies were carried out in simulated intestinal fluids (biorelevant media) and their cytocompatibilty in human intestinal cells [cancer colon (Caco-2)].

2. Materials and Methods

2.1 Materials

Ibuprofen (IBU) was purchased by Sigma-Aldrich (St. Louis, MO, USA). Mesoporous carbon aerogels CA10 and CA20 were obtained from the Bavarian Centre for Applied Energy Research (ZAE Bayern, Germany) association, in the form of macroscopic cm-sized monoliths. Ethanol was purchased by Chem-Lab NV, Industriezone “De Arend” 2, B-8210 Zedelgem, Acetonitrile-HPLC (Chromasolv

gradient grade, for HPLC, ≥ 99,9 %), Sodium Chloride (NaCl) was purchased by E. Merck, D-G100, Darmstadt, F.R. Germany. Biorelevant media were purchased from biorelevant.com (UK).

2.2 Physicochemical characterization of carbon aerogels and their complexes with IBU

2.2.1 Loading studies

37.5 mg of IBU were dissolved in 0.5 mL of EtOH and were added in 2 mL of EtOH containing 75 mg of each carbon material. Each mixture was sonicated for 30 sec and kept under magnetic stirring overnight at room temperature in a closed container. The samples were centrifuged at 5,560 *g* at room temperature for 30 min and the supernatants were collected and analyzed by HPLC. Carbon loaded samples were dried and stored at 40 ^{o}C for 24 h and then kept under vacuum for 24 h, prior to further analysis.

2.2.2 Determination of loading efficiency

Two (2) mg of each formulation were dispersed in 10 mL of EtOH and left under stirring overnight. After centrifugation at 5,560 *g* for 30 min, supernatants were collected and further analyzed by HPLC.

2.2.3 High Resolution-Transmission Electron Microscopy (HR-TEM) analysis

TEM measurements were performed on the CAs, in order to investigate possible morphological characteristics of these materials. Samples suitable for TEM were prepared by drop casting the ethanol solution containing the CAs particles on holey carbon-coated copper grids. HRTEM images and selected area electron diffraction

(SAED) patterns were acquired using a Tecnai G2 electron microscope operated at 200 kV.

2.2.4 Pore properties

The pore properties of the two carbon hosts (before and after loading with IBU) were deduced from N_2 sorption/desorption isotherms at 77 K that were collected using a commercial volumetric gas adsorption system (Autosorb-1-MP, Quantachrome). The samples (~50 mg) were appropriately outgassed (~ 24 h at 50 °C) under high vacuum (10-6 mbar) prior to each measurement, while ultra-pure N_2 (99.9999 %) was used. The specific surface area values were calculated by the Brunauer–Emmett–Teller (BET) method, whereas the pore size distributions were deduced based on the Barrett-Joyner-Halenda (BJH) approximation. Total pore volumes were estimated from the amount of N_2 adsorbed at a relative pressure of 0.99.

2.2.5 Differential Scanning Calorimetry (DSC)

DSC analysis of the samples was carried out with a DSC instrument (DSC 204 F1 Phoenix, NETZSCH) using a heating rate of 10 ^{o}C/min under a nitrogen purge of 70 mL/min from 20 ^{o}C to 120 ^{o}C.

2.2.6 X-ray diffraction (XRD)

Crystallinity of the samples was evaluated with XRD analysis performed on an XRD Bruker D8-Advance apparatus operated at 40 kV and 40 mA, Cu Ka1 radiation, on a scanning rate of 0.35 sec/step.

2.2.7 X-ray photonelectron spectroscopy (XPS) studies

XPS measurements were conducted in order to verify and investigate the existence of the IBU within the CA10 and CA20 carriers. The pertinent studies were performed in an Ultra High Vacuum (UHV) chamber ($P < 10^{-9}$ mbar) equipped with a SPECS LHS-10 hemispherical electron analyzer. The XPS measurements were carried out at room temperature using unmonochromatized AlKa radiation under conditions optimized for maximum signal (constant ΔE mode with pass energy of 36 eV giving a full width at half maximum (FWHM) of 0.9 eV for the Au 4f7/2 peak). The analyzed area was an ellipse with dimensions 2.5 x 4.5 mm^2. The XPS core level spectra were analyzed using a fitting routine, which can decompose each spectrum into individual mixed Gaussian-Lorentzian peaks after a Shirley background subtraction. Errors in the quantitative data were found in the range of 10 % (peak intensities) while the accuracy for Bes assignments is ± 0.1eV. The samples were pressed in an in foil. Non-loaded CA10 and CA20 samples onto in foil as well as pure in foil were also measured in order to compare with the carrier's and to subtract the substrate contribution.

2.2.8 Surface charge studies

ζ-potential measurements were carried out with an instrument Zetasizer Nanoseries, Nano-ZS analyzer, Malvern Instruments, UK at room temperature with source of radiation 4Mw He-Ne Laser, 633 nm, at an angle 90^o. Empty and drug loaded formulations were dispersed in distilled water and subsequently were measured for their surface charge properties.

2.3 In vitro studies

2.3.1 Release studies in simulated intestinal fluids

Release studies were performed in glass vials under gentle agitation in simulated intestinal fluids. Fasted intestinal simulated fluids (FaSSIF) [BS (sodium taurocholate), 3 mM ; phospholipid (lecithin) 5 mM ; Sodium dihydrogen phosphate (mM) 28,65; hydrochloric acid, sodium chloride 105,85 mM ; Osmolarity (mOsmol/kg), ~ 270 ; Buffer capacity (mEq/pH/l), ~ 12; pH 6.5] and fed intestinal simulated fluids ((FeSSIF) [BS (sodium taurocholate), 15,75 mM ; phospholipid (lecithin) 3,75 mM ; acetic acid, 144,05, hydrochloric acid, sodium chloride 203,18 mM ; Osmolarity (mOsmol/kg), ~ 670 ; Buffer capacity (mEq/pH/l), ~ 72 ; pH 5.0] were utilized reflecting the physiological conditions in human gastrointestinal tract [Galia et al. 1998].

In detail, 20 mL of FaSSIF or FeSSIF media were deposited in glass vials containing 6.3 mg of drug loaded CA10 and 5 mg CA20 (drug target of 1149 μg of IBU) particles under stirring at 37 º C. Samples of 1 mL were withdrawn at predetermined time points (0, 5, 10, 15, 30, 45, 60, 90 and 180 min), followed by immediate replacement of media. Samples were diluted 1:1 in ACN and centrifuged at 4,500 rcf for 20 min. All samples were filtered through 0.45 μm PVDF filters and the supernatants were analyzed by HPLC.

2.3.2 HPLC analysis

Drug content was quantified using an HPLC system consisting of a LC-10 AD VP pump, an autosampler model SIL-20A HT equipped with a 100 μL loop and a UV-Vis detector model SPD-10A VP (SHIMADZU). Class VP Chromatography data system version 4.3 (SHIMADZU) was the software used. UV detector was set at 230 nm for the detection of ibuprofen. A Discovery® RP Amide C16, (150 x 4.6) mm, 5 μm was the selected column. The mobile phase consisted of ACN: Water 25 mM KH2PO4

(pH=3) 45:55 v/v, with a 1.1 mL/min flow rate. For the determination of the drug content 30 μL were used as injection volume with a runtime of 16 min. The calibration curves for IBU were linear (r^2>0.999) in the range of 1 - 20 μg/mL.

2.4 Cytotoxicity studies

2.4.1 Caco-2 cell cultures

Cell culture reagents Dulbecco's Modified Eagle's Medium (DMEM,), Fetal Bovine Serum (FBS), Penicillin and Streptomycin (PS), MEM Non-Essential Amino Acids (NEAA), trypsin were obtained from GIBCO whereas the 3-(4,5-Dimethyl-2-thiazolyl)-2,5-diphenyl-2H-tetrazolium bromide (MTT) colorimetric assay kit was purchased from Trevigen.

Caco-2 cells were grown at 37 °C in a humidified atmosphere containing 5 % v/v CO2. The culture medium consisted of DMEM, supplemented with 10 % v/v FBS, penicillin and streptomycin S (100 μg/mL of each) and 1 % v/v non-essential amino acids (NEAA). In stock cultures, the medium was changed every other day. Caco-2 cultures at passages 41 - 44 were used in the experiments described and cells were sub-cultured by trypsinization in tissue culture flasks.

2.4.2. Cytotoxicity assessment of CA10 and CA20 in Caco-2 cells

Initially, the *in vitro* cytotoxicity effects of both CAs in Caco-2 was assessed by the MTT cell proliferation assay [Hidalgo et al. 1989]. Cell cultures of density 10^4 cells per well were incubated with increasing concentration (0, 25, 50, 100, 250 and 500 μg/mL) of CA10 and CA20 for 48 h and absorbance measurements were taken at 600 nm. However, the carbon material was attached to the cell membranes which in turn

affected the accuracy of the readings (absorbance values). For this reason the direct count of cell numbers in cultures was carried out in an attempt to evaluate the effect of CA10 and CA20 on Caco-2 cell proliferation. Cells were seeded in a 24 -well plate at an initial density of 10^5 cells/mL. After cell attachment (~3 h), the material suspensions (0, 25, 50, 100, 250 and 500 μg/mL) were added to the culture and cells were incubated for 48 h. Then, cells were detached by trypsinization and the number of cells in culture was determined using a Neubauer plate. Simultaneously, the cellular death was assessed using trypan-blue dye exclusion method [Strober, 2001]. Then cell proliferation capacity in treated cultures was expressed as percentage (%) of that for control untreated cells.

2.4.3 Stability studies

The stability of the CA samples in simulated intestinal fluids was assessed by means of TEM. Carbon powder (approximately 4 mg) were added in 10 mL of FaSSIF and FeSSIF media and incubated for 2 h at 37 ^{o}C. Samples were processed for TEM by drop casting the aqueous dispersions on holey carbon-coated copper grids.

2.4.4 Optical microscopy studies

Furthermore, to obtain a better morphology of cell cultures exposed to material suspensions, concentrations of 50 μg/mL of CA10 and CA20 was chosen for the exposure of cultures for 3 h, 24 h and 48 h, whereas the cells were washed with PBS (pH 7.4) before their microscopic evaluation.

2.4.5 Statistical analysis

Statistics were performed by paired t-test. A significance level of $p < 0.05$ denoted significance.

3. Results and Discussion

3.1 Characterization of the carriers and their complexes with IBU

3.1.1 TEM studies

TEM images of the raw materials are presented in Figure 1. The typical tortuous carbon structure of the aerogels is present in all images (Figure 1A, B and C) [Wu et al. 2006] Moreover mesopores of different sizes could be identified in CA20 (Figure 1B, indicated by the red arrows), a feature that it is not so obvious in the CA10 sample [Zhang et al. 2005b]. Particularly for CA20 sample the presence of nanosized crystalline graphite can be observed (Figure 1C) [Maldonado-Hodar et al. 2000]. This graphitic structure is a byproduct and can probably be attributed to the synthesis conditions which were used in order to prepare the samples.

3.1.2 N_2 adsorption/desorption studies

The N_2 adsorption - desorption isotherms for the CA10 and CA20 carbons presented in Figure 2A and B, are of type IV (based on IUPAC classification) with abrupt condensation-evaporation hysteresis loops, characteristic of the presence of mesopores. The pore analysis based on the respective data showed that the mean pore size of CA10 and CA20 is 8 and 13.5 nm, respectively (Figure 2C and D) whereas the pore size of the loaded carbons is practically unaltered (7.9 and 12.9 nm). As such, although the two carbons possess similar specific surface areas (around 750 m^2/g) as shown in Table 1, CA20 offers almost the double pore volume (total pore volume =

1.36 cm^3/g compared to 0.78 cm^3/g for the case of CA10), a critical parameter of particular interest for the efficiency of the encapsulation of the active compound (Table 1).

A significant reduction in specific surface area (m^2/g) of approximately 55 % and 59 % and in pore volume (cm^3/g) of approximately 22 % and 26 % were observed for the CA10 - IBU and CA20 - IBU samples, respectively, indicating successful drug loading by deposition within the pores or on the external surface of the carbon materials affecting further incorporation of the drug in the pores network. These differences were more pronounced in the case of CA20 - IBU which might be attributed to the higher percentage of drug encapsulation for the CA20 aerogel compared to CA10 (also having lower total pore volume).

3.1.3 DSC Thermographs

DSC thermograms (Figure 3A and B) showed the characteristic peak of IBU at 78.5 ^{o} C, attributed to its melting point (T_m = 77 - 78 ^{o}C). However for the drug loaded formulations no thermal activity, ascribed to drugs crystals, could be detected which may indicate that the drug is in an amorphous state. The only prominent feature of the DSC thermograms, is a broad endotherm in the region of 60 - 90 °C for both carbons which might be attributed to moisture.

3.1.4 X-ray diffraction (XRD) studies

The X-ray diffractograms of empty and drug loaded carbons are shown in Figure 3C and 3D, respectively. The crystalline form of the drug exhibited multiple diffraction peaks in the XRD pattern. IBU loaded CA10 sample presented no distinctive diffraction peaks, indicating the inclusion of the drug within the carrier's pores in a

non-crystalline state. It has been suggested that crystallization occurs inside the pores of materials with diameters to molecular size ratios more than 20 [Shen, S-C et al. 2010; Sliwinska-Bartkowiak et al. 2001]. Given that the dimensions of IBU is approximately 1.0 x 0.6 nm it may be assumed that the drug is in an amorphous state in the pores.

3.1.5 XPS analysis

The spatial distribution of the drug onto the surface of the carbons was assessed by means of XPS. The survey scans of the empty and drug loaded CA10 and CA20 on In foil (ESI, Figure S1) reveals the presence of carbon, oxygen and In peaks from the substrate. Figure 4 shows the C1s core level spectra of the empty and drug loaded CA10 and CA20 surfaces. The C1s spectra were analysed and assigned to functional groups according to the literature (Karavasili et al 2016).

No differences at binding energies and at the relative components intensity ratio observed in the C1s spectra between the empty and the drug loaded CA -10 (Figure 4A and C). On the contrary, in the IBU-CA20 sample (Figure 4D) the intensity of the C-C component is more pronounced relative to the other components (C-O, C=O, COOH) than in the CA20 sample (Figure 4B). Moreover, the binding energy of the C-C component of CA20-IBU sample is at 284.4eV (assigned in double C=C bonds) while in the other three samples is at 284.7 eV assigned to hydrocarbons.

This is an indication of a pronounced presence of C=C bonds (sp2 hybridization) which are present in IBU [Sopinskyy et al. 2014] in the CA20-IBU sample. From the total intensity of the C1s and O1s peaks the atomic ratio O/C can be derived. The contribution in the O1s from the in substrate is subtracted. The atomic ratios for different formulations are shown in Table 1. For the empty CA10, CA20 and the

loaded IBU-CA10 the atomic ratio is approximately 0.20, whereas for the IBU - CA20 is 0.14 as illustrated at Table 1. Notably the nominal ratio O/C of IBU is 0.15. The presence of oxygen in the carriers is mainly due to hydroxides because of sample exposure to the atmosphere. The atomic ratio O/C in the IBU-CA20 is close to the IBU. This result in combination with the binding energy of the C-C main component is a clear indication of the presence of IBU onto the CA20 surface. On the contrary, the O/C ratio in the IBU-CA10 is close to the value of the empty carrier indicating the absence of IBU on the CA-10 surface. Taking into account that XPS is a surface sensitive technique, the absence of the drug in the CA10 sample is probably due to the drug incorporation on the CA10 pores and not on the surface. Notably in the O1s spectra the contribution of the substrate (In foil covered with native oxide) is intense. The peak analyzed into four components which were assigned to functional groups according to the literature and to substrate (In-O) [Karavasili et al. 2016] are shown in ESI, Figure S1.

3.1.6 ζ-potential studies

Both carbon materials possess a negative charge as evident from Table 1. Consistent with the considerable accumulation of IBU onto the surface of the carbons the ζ-potential of IBU loaded materials (-27.0 ± 0.55 mV for CA10 and -41.0 ± 3.55 for CA20 mV) is markedly lower (t-test, $p<0.05$) than that of corresponding IBU-free structures (-22.2 ± 0.76 mV for CA10 and -10.7 ± 2.68 mV for CA20). Differences (t-test, $p<0.05$) for IBU-CA10 carbons are less pronounced which may be attributed to the lower loading capacity of CA10 compared to its CA20 congener.

3.2 In vitro studies

3.2.1 Dissolution studies in simulated intestinal fluids

The amount of drug incorporated into the carbons from the loading efficiency studies was 18.2 ± 0.77 and 22.9 ± 1.05 (% w/w) for CA10 and CA20, respectively. The higher payload capacity of the CA20 aerogel might be attributed to its larger mean pore size and total pore volume compared to CA10 (Table 1).

Drug release profiles of IBU from CA10 and CA20 in FaSSIF and FeSSIF media are presented in Figure 5 A & B. In FaSSIF (pH 6.5) conditions significantly higher amount of drug was solubilized compared to FeSSIF (pH 5.0) conditions. This is in accordance with previous studies where IBU release was highly dependent on the buffer composition and pH values [Levis et al. 2003; Sanchez-Sanchez et al. 2015]. In FaSSIF media the release of drug reached its maximum value of approximately 14 % for CA20 and approximately 45 % for CA20 with 5 min (Figure 5A). In contrast, in FeSSIF media IBU displayed prolonged release at the same timescale where approximately 8 % of the drug was released from CA10 and approximately 23 % of the drug was released from its CA20 congener (Figure 5B). In both media the faster release of IBU from CA20 might be attributed to the presence of a larger amount of the drug onto its surface as also suggested by the XPS and ζ-potential studies. Both formulations did not reach 100 % of dissolution within 120 min.

3.2.2 Cytocompatibility of CA10 and CA20 and cellular morphology on the Caco-2 cell culture

Caco-2 cell cultures incubated for 24 h with increasing concentrations of CA10 and CA20 materials did not show any statistically significant reduction of cell growth (t-

test, $p<0.05$), nor exhibited any increase of cell death compared to a control untreated culture (Figure 5C). However, cell cultures incubated for up to 48 h with the materials demonstrated a slight inhibition of cell growth, where cultures incubated with the maximum 500 μg/mL concentration of CA10 and CA20 demonstrated an inhibition of cell growth of about 40 % compared to control (t-test, $p>0.05$) (Figure 5D) an indication that these material might considered potentially cytotoxic at these concentrations (ISO 10993-5). Importantly, this effect does not seem to be dose-dependent, especially for cells incubated with CA20 material, and could be attributed to mechanical obstruction of the carbon materials to cell proliferation potential. Based on this behavior, the IC_{50} value of both materials in Caco-2 cells is much higher than the tested carbon aerogels concentrations (500 μg/mL).

Moreover, cell viability expressed as the proportion of dead cells measured in treated cell cultures was almost identical to that of the control (data not shown). The results obtained in the current study are in good agreement with previous studies where ordered mesoporous carbons (OMCs) didn't exhibit any toxicity when tested in Caco-2 cells line [Karavasili et al. 2013]. The low toxicity of mesoporous carbons has been documented to another cell line as well (HeLa) in previous studies further corroborating their cytocompatility [Kim et al. 2008; Karavasili et al. 2013; Gencoglu et al. 2014].

3.2.3 Stability studies

Previous studies have shown that exposure to simulated body fluids [Choi et al. 2015] or in the acidic environment of the stomach [Fatouros et al. 2011; Spanakis et al. 2014] might induce erosion of the inner structure of the carriers an indication of degradation which in turn might alter the release behavior of the active. Typical images of the two carbon aerogels incubated for 2 h with FASSIF and FESSIF media are presented in Figure 6. No defects in the morphology or in the structure of the

carbons could be identified upon exposure to these media (Figure 6A & B). Notably in Figures 6C & D the presence of mixed micelles with diameters approximately 5 nm, originating from the medium, could be detected. These results imply that the dominant factor for the release of IBU from the carbons is solely attributed to the textural properties and their encapsulation capacity (pore size).

3.2.4 Light microscopy studies

Optical microscopy allowed the visualization of untreated cells as circular-shaped structures (Figure 7). Exposure to the carbons at a concentration of 50 μg/mL (for 3h) did not appear to affect the cell morphology (Figure 7). Furthermore, it was observed that upon incubation of Caco-2 cells with CA10 and CA20 materials cellular uptake was achieved early. In particular, their cytoplasmic accumulation was evidenced as early as after 3 h of incubation (Figure 7) even after washing of the cells. Moreover exposure to carbon aerogels with concentrations up to 500 μg/mL did not appear to affect cell morphology (data not shown).

4. Conclusions

The two carbon aerogels investigated in this study have similar architectures but different pore sizes and exhibit markedly different release profiles for the same drug in simulated intestinal fluids. The cytocompatibility studies show that carbon aerogels are non-toxic to human cells *in vitro* underlining their significant potential for *in vivo* applications.

Acknowledgements

The authors appreciate financial support from the European Union under the Seventh Framework Program (Integrated Infrastructure Initiative No. 262348 European Soft Matter Infrastructure, ESMI).

References

Antonietti, M., Fechler, N., Fellinger, T.-P., 2014. Carbon aerogels and monoliths: control of porosity and nanoarchitecture *via* sol-gel routes. Chem. Mater. 26 , 196 - 210.

Choi, Y., Lee, J.E., Lee, J.H., Jeong, J.H., Kim, J. 2015. A biodegradation study of SBA -15 microparticles in simulated body fluid and *in vivo*. Langmuir. 31, 6457 - 6462.

Fatouros, D.G., Douroumis, D., Nikolakis, V., Ntais, S., Moschovi, A.M., Trivedi, V., Khima, B., Roldo, M., .Nazar, H., Cox, P.A., 2011. *In vitro* and *in silico* investigations of drug delivery via zeolite BEA. J. Mater. Chem. 21, 7789 - 7794.

Galia, E., Nicolaides, E., Hörter, D., Löbenberg, R., Reppas, C., Dressman, J.B., 1998. Evaluation of various dissolution media for predicting in vivo performance of class I and II drugs. Pharm. Res. 15, 698 - 705.

Gao, Y., Zhu W., Liu, J., Di, D., Chang, D., Jiang, T., Wang S., 2015. A geometric pore adsorption model for predicting the drug loading capacity of insoluble drugs in mesoporous carbon Inter. J. Pharm. 485, 15 25-30.

Gencoglu, M.F., Spurri, A., Franko, M., Chen, J., Hensley, D.K., Heldt, C.L., Saha, D., 2014. Biocompatibility of soft-templated mesoporous carbons. ACS Appl. Mater. Interfaces. 6, 15068 - 15077.

Hidalgo, I.J., Raub, T.J., Borchardt, R.T., 1989. Characterization of the human-colon carcinoma cell-line (Caco-2) as a model system for intestinal epithelial permeability. Gastroenterology. 96, 736 - 749

Horcajada, P., Chalati, T., Serre, C., Gillet, B., Sebrie, C., Baati, T., Eubank, J. F., Heurtaux, D., Clayette, P., Kreuz, C., Chang, J.S., Hwang, Y.K., Marsaud, V., Bories, P.N., Cynober, L., Gil, S., Férey, G., Couvreur, P., Gref, R., 2010. Porous

metal-organic-framework nanoscale carriers as a potential platform for drug delivery and imaging. Nat. Mater. 9, 172 -178.

International Standard ISO 10993-5 Biological evaluation of medical devices- Part 5 : Tests for *in vitro* toxicity

Karavasili, C., Amanatiadou, E.P., Sygellou, L., Giasafaki, D., Steriotis, T., Charalambopoulou, G., Vizirianakis, I.S., Fatouros, D.G., 2013. Development of new drug delivery systems based on ordered mesoporous carbons: characterisation and cytocompatibility studies. J. Mater. Chem. B. 1, 3167 - 3174.

Karavasili, C., Bouropoulos, N., Sygellou, L., Amanatiadou, E.P., Vizirianakis, I.S., Fatouros, D.G., 2016. PLGA/DPPC/trimethylchitosan spray-dried microparticles for the nasal delivery of ropinirole hydrochloride: *in vitro*, *ex vivo* and cytocompatibility assessment. Mater. Sci. Eng. C 59, 1053-1062.

Kim, T.W., Chung, P.W., Slowing, I.I., Tsunoda, M., Yeung, E.S., Lin, V.S., 2008. Structurally ordered mesoporous carbon nanoparticles as transmembrane delivery vehicle in human cancer cells. Nano Lett. 8, 3724 - 372.

Leuner, C, Dressman, J., 2000. Improving drug solubility for oral delivery using solid dispersions, Eur J. Pharm. Biopharm. 50, 47 - 60.

Levis, K.A., Lane, M.E., Corrigan, O.I., 2003. Effect of buffer media composition on the solubility and effective permeability coefficient of ibuprofen. Int. J. Pharm. 253, 49 - 59.

Maldonado-Hodar, F., Moreno-Catilla, C., Rivera-Utrilla, J., Hanzawa, Y., Yamada, Y., 2000. Catalytic Graphitization of carbon aerogels by transition metals. Langmuir. 16, 4367- 4373.

McKinlay, A.C., Morris, R.E., Horcajada, P., Férey, G., Gref, R., Couvreur, P., Serre, C., 2010. BioMOFs: metal-organic frameworks for biological and medical applications. Angew. Chem. Int. Ed. Engl. 49, 6260 - 6266.

Mellaerts, R., Jammaer, J.A.G., Van Speybroeck, M., Chen, H., Van Humbeeck, J., Augustijns, P., Van den Mooter, G., Martens, J.A., 2008. Physical state of poorly water soluble therapeutic molecules loaded into SBA-15 ordered mesoporous silica carriers: a case study with itraconazole and ibuprofen. Langmuir. 24, 8651 - 8659.

Pekala, R.W., Alviso, C.T., Kong, F.M., Hulsey, S.S., 1992. Aerogels derived from multifunctional organic monomers. J. Non-Crystal. Solids 145, 90 - 98.

Salonen, J., Laitinen, L., Kaukonen, A., Tuura, J., Bjorkqvist, M., Heikkilä, T., Vähäheikkilä, K., Hirvonen, J., Lehto, V.P., 2005. Mesoporous silicon microparticles for oral drug delivery: loading and release of five model drugs. J. Control. Release. 108, 362 - 374.

Sanchez-Sanchez, A., Suarez-Garcia, F., Martinez-Alonso, A., Tascon, J.M.D., 2015. pH-responsive ordered mesoporous carbons for controlled release of ibuprofen. Carbon. 94, 152 - 159.

Santos, H.A., Peltonen, L., Limnell, T., Hirvonen, J., 2013. Mesoporous materials and nanocrystals for enhancing the dissolution behavior of poorly water-soluble drugs. Curr. Pharm. Biotechnol. 14 : 926 - 938.

Shen, S-C., Ng, W.K., Chia, L., Dong, Y-C., Tan, R.B.H. 2010. Stabilized amorphous state of ibuprofen by co-spray drying with mesoporous SBA-15 to enhance dissolution properties. J. Pharm. Sci. 99, 1997 - 2007.

Sliwinska-Bartkowiak, M., Dudziak, G., Gras, R., Sikorski, R., Radhakrishnan R., Gubbins, K.E., 2001. Freezing behavior in porous glasses and MCM-41. Colloids Surf. A: Physic. Eng. Asp. 187 - 188, 523 - 529.

Sopinskyy, M., Khomchenko, V., Strelchuk, V., Nikolenko, A., Olchovyk, G., Vishnyak, V., Stonis, V., 2014. Possibility of graphene growth by close space sublimation. Nanosc. Res. Let. 9:182.

Spanakis, M., Bouropoulos, N., Theodoropoulos, D., Sygellou, L., Ewart, S., Moschovi, A.M., Siokou, E., Niopas, I., Kachrimanis, K., Nikolakis, V., Cox, P.A., Vizirianakis, I.S., Fatouros, D.G., 2014. Controlled release of 5-flourouracil from microporous zeolites. Nanomedicine. 10 : 197 - 205.

Strober, W., 2001. Trypan blue exclusion test of cell viability. Curr Protoc Immunol. Appendix 3:Appendix 3B

Vallet-Regí, M., Rámila, A., del Real, R.P., Pérez-Pariente, J., 2001a. A new property of MCM-41: drug delivery system. Chem. Mater. 13 : 308 - 311.

Vallet-Regí, M., Balas F., Arcos D., 2007b. Mesoporous materials for drug delivery. Angew. Chem. Int. Ed. Engl. 46 : 7548 - 7558.

Wan, L., Wang X., Zhu, W., Zhang, C. Song A., Sun C., Jiang T., Wang S., 2015. Folate-polyethyleneimine functionalized mesoporous carbon nanoparticles for enhancing oral bioavailability of paclitaxel. Inter. J. Pharm. 484 : 207- 217.

Wu, D., Fu, R., Dresselhaus, M.S., Dresselhaus, G., 2006. Fabrication and nano-structure control of carbon aerogels via a microemulsion-templated sol-gel polymerization method. Carbon. 44, 675 - 681.

Zhang, Y., Zhao, Q., Zhu, W., Zhang, L., Han, J., Lin, Q., Ai, F., 2015a. Synthesis and evaluation of mesoporous carbon/lipid bilayer nanocomposites for improved oral delivery of the poorly water-soluble drug, nimodipine. Pharm. Res. 32 , 2372 - 2383.

Zhang, Y., Kang, D., Aindow, M., Erkey, C. J., 2005. Preparation and characterization of ruthenium/carbon aerogel nanocomposites via a supercritical fluid route. J. Phys. Chem. B. 109, 2617 - 2624.

Zhao, P., Wang, L., Sun, C., Jiang, T., Zhang, J., Zhang, Q., Sun, J., Deng, Y., Wang, S., 2012. Uniform mesoporous carbon as a carrier for poorly water soluble drug and its cytotoxicity study. Eur. J. Pharm. Biopharm. 80, 535 - 543.

FIGURE LEGENDS

FIGURE 1: TEM images of the samples CA10 and CA20. **A**. Low magnification TEM image of CA10. The material is amorphous and can be confirmed from the SAED pattern. **B**. Low magnification TEM image of CA20, where mesopores of various sizes can be observed, indicated by the red arrow. The material is amorphous and can be confirmed from the SAED pattern. **C**. HRTEM image of CA20 with the characteristic crystalline graphite structure.

FIGURE 2: **A**. N_2 sorption/desorption isotherms (77 K) of the carbon aerogels CA10 and (**B).** CA20. Pore size distributions of the carbon aerogels CA10 (**C**) and CA20 (**D**).

FIGURE 3: DSC thermograms of (**A**) IBU, CA10 and CA10 - IBU, (**B**) IBU, CA20 and CA20 -IBU. X-ray difractogramms of (**C**) IBU, CA10 and CA10-IBU, (**D**) IBU, CA20 and CA20 - IBU.

FIGURE 4: Deconvoluted C1s and core level spectra of loaded (**A**) IBU - CA10 and (**B**) IBU - CA20 (**C**) IBU - CA10 and (**D**) IBU - CA20 samples pressed on In foil.

FIGURE 5: Release studies of IBU from loaded carbon aerogels in (**A**) FaSSIF and (**B**) FeSSIF simulated intestinal fluids, (**C**) Cell growth (Caco-2 cell lines) after 24 h of incubation as a function of the CA10 and CA20, (**D**) Cell growth (Caco-2 cell lines) after 48 h of incubation as a function of the CA10 and CA20, error bars are mean ± S.D. of three experiments. Asterisk at high concentrations (500 μg/mL at 48 h indicated that carbon aerogels exhibited cytotoxicity).

FIGURE 6: TEM images of the (**A**) CA10 carbons incubated with FaSSIF media. (**B**) CA20 carbons incubated with FaSSIF media. (**C**) CA10 carbons incubated with FeSSIF media. (**D**) CA20 carbons incubated with FeSSIF media.

FIGURE 7: Light microscopy images of Caco-2 cells of control and carbon treated materials (50 μg/mL of CA10 and CA20) for 3h and then washed twice with PBS.

FIGURE 1

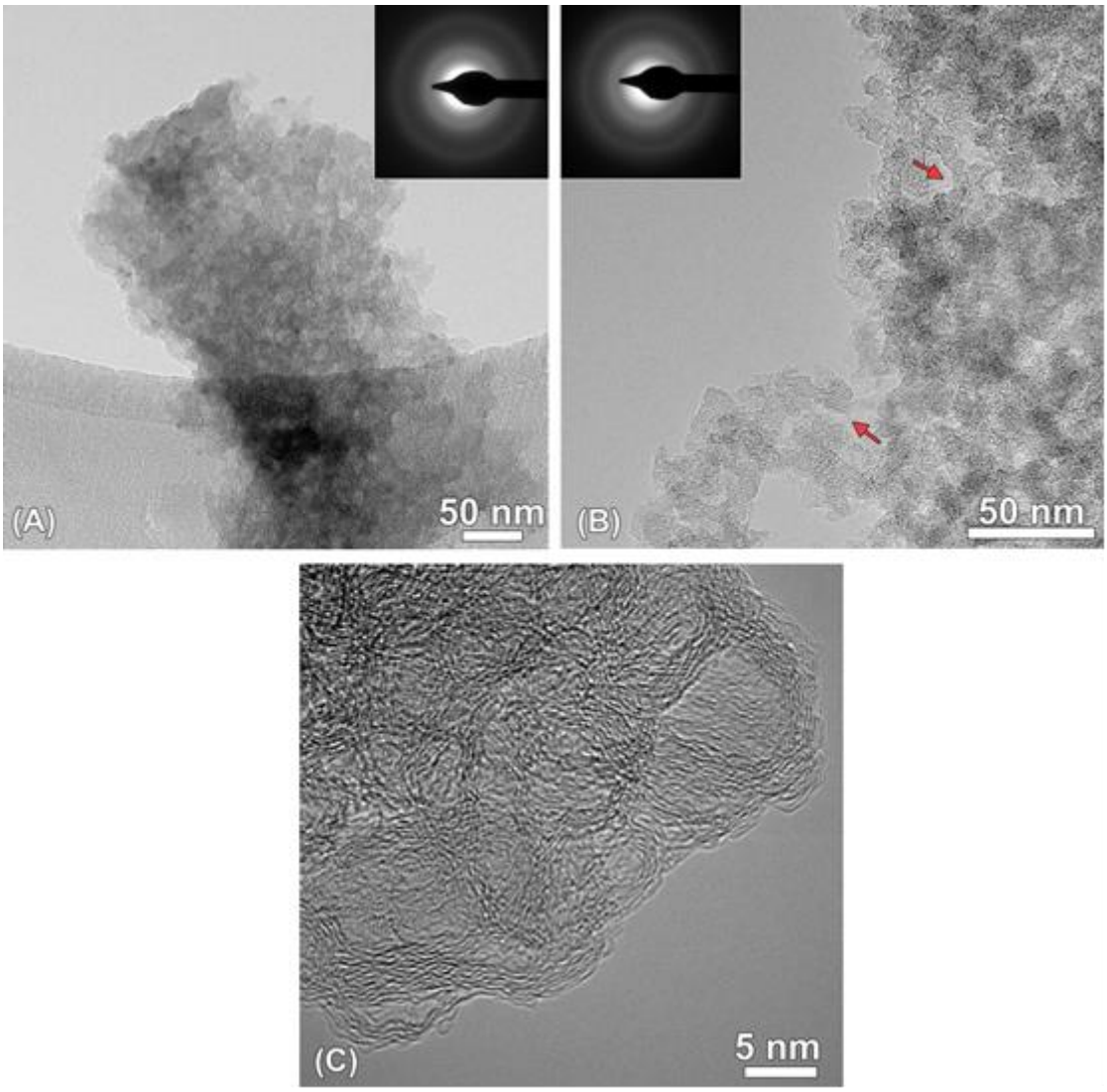

FIGURE 2

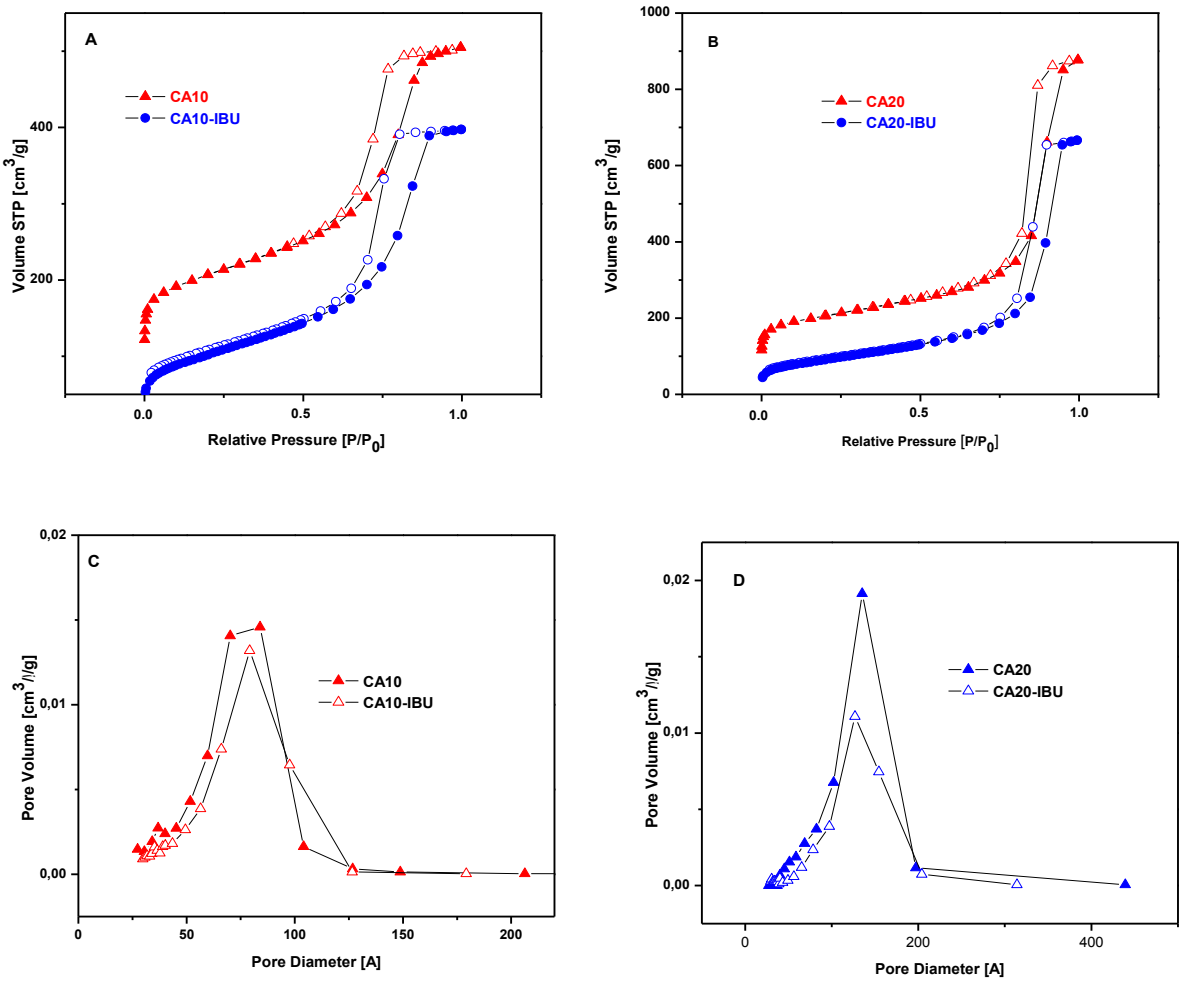

FIGURE 3

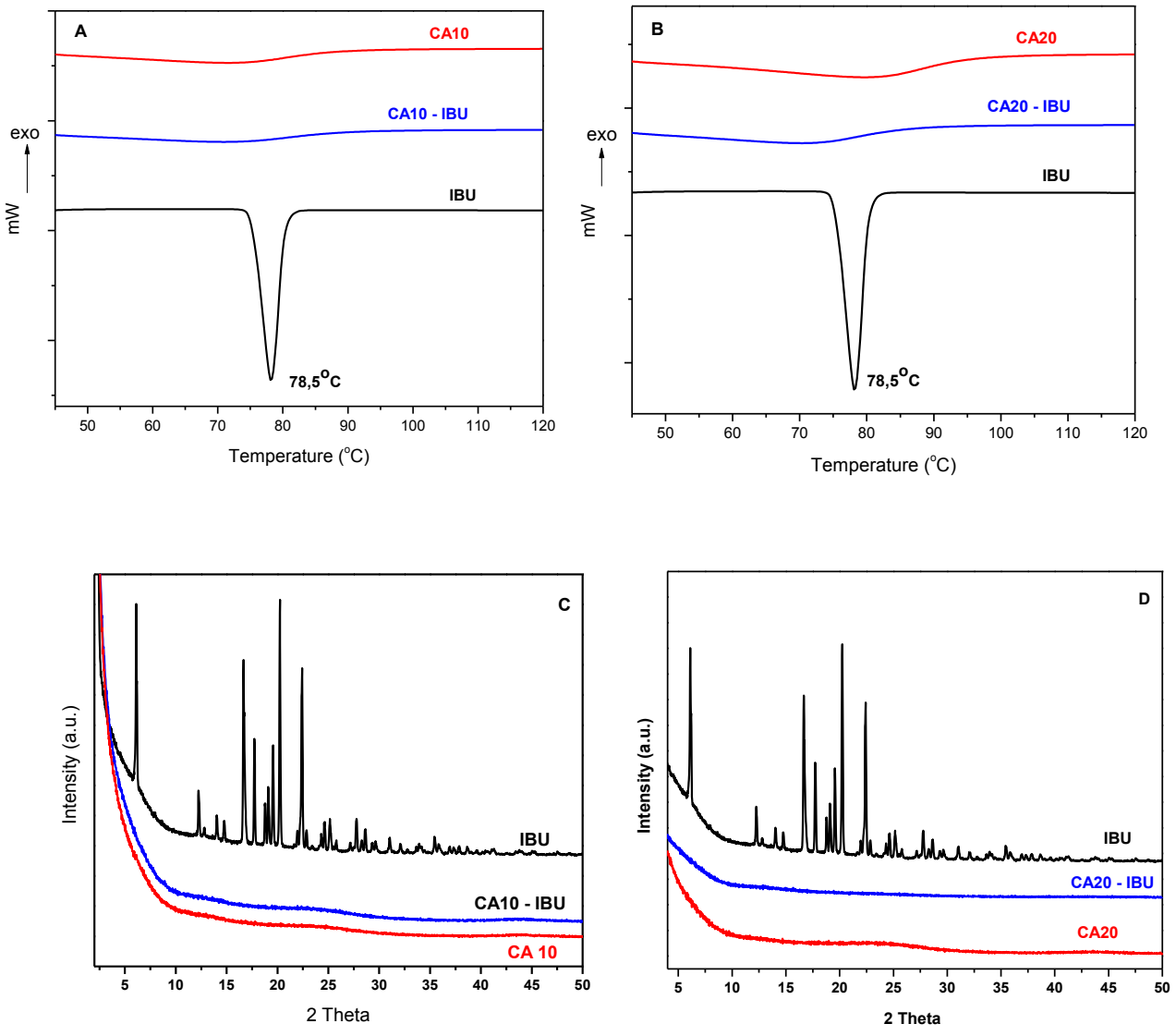

FIGURE 4

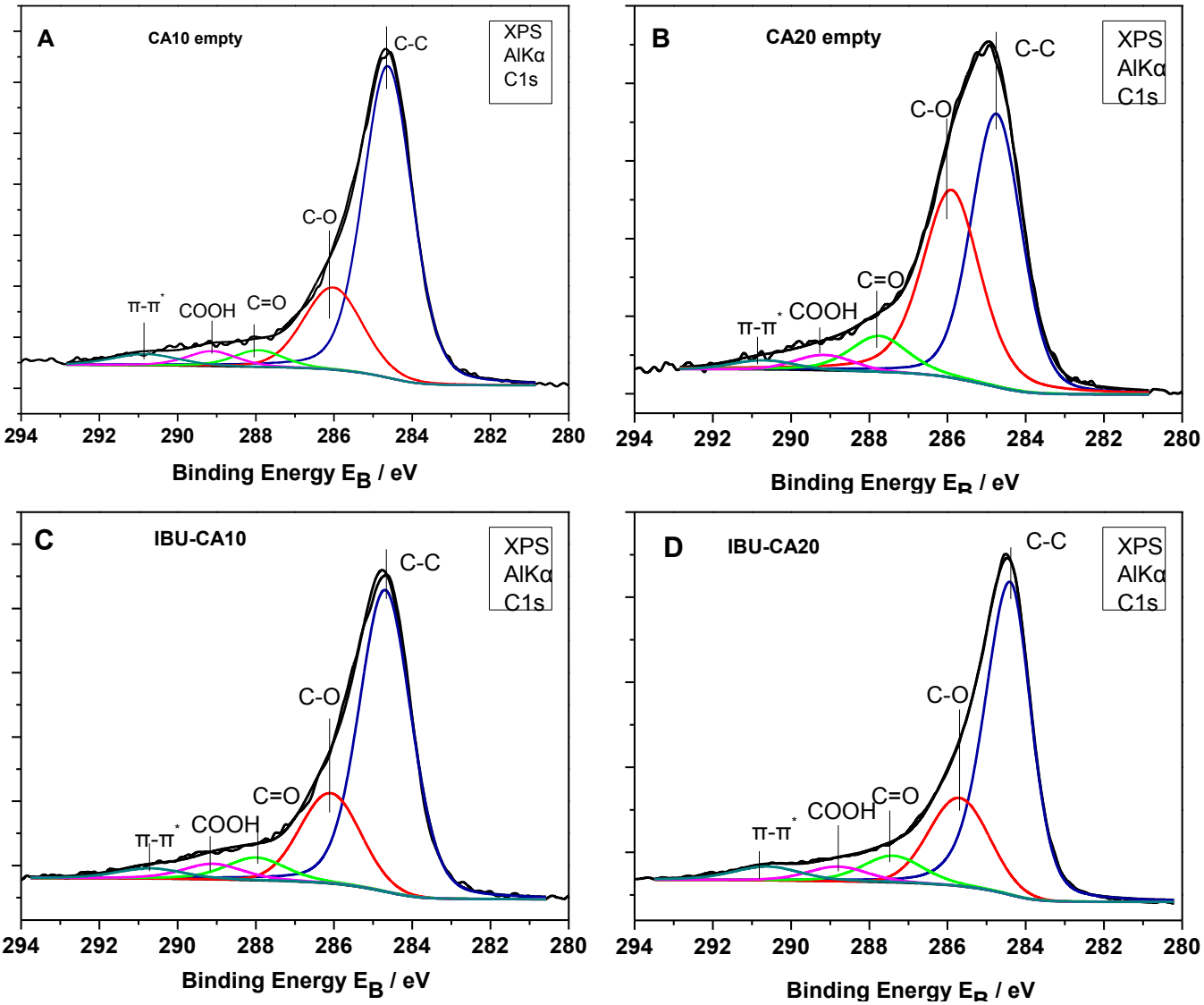

FIGURE 5

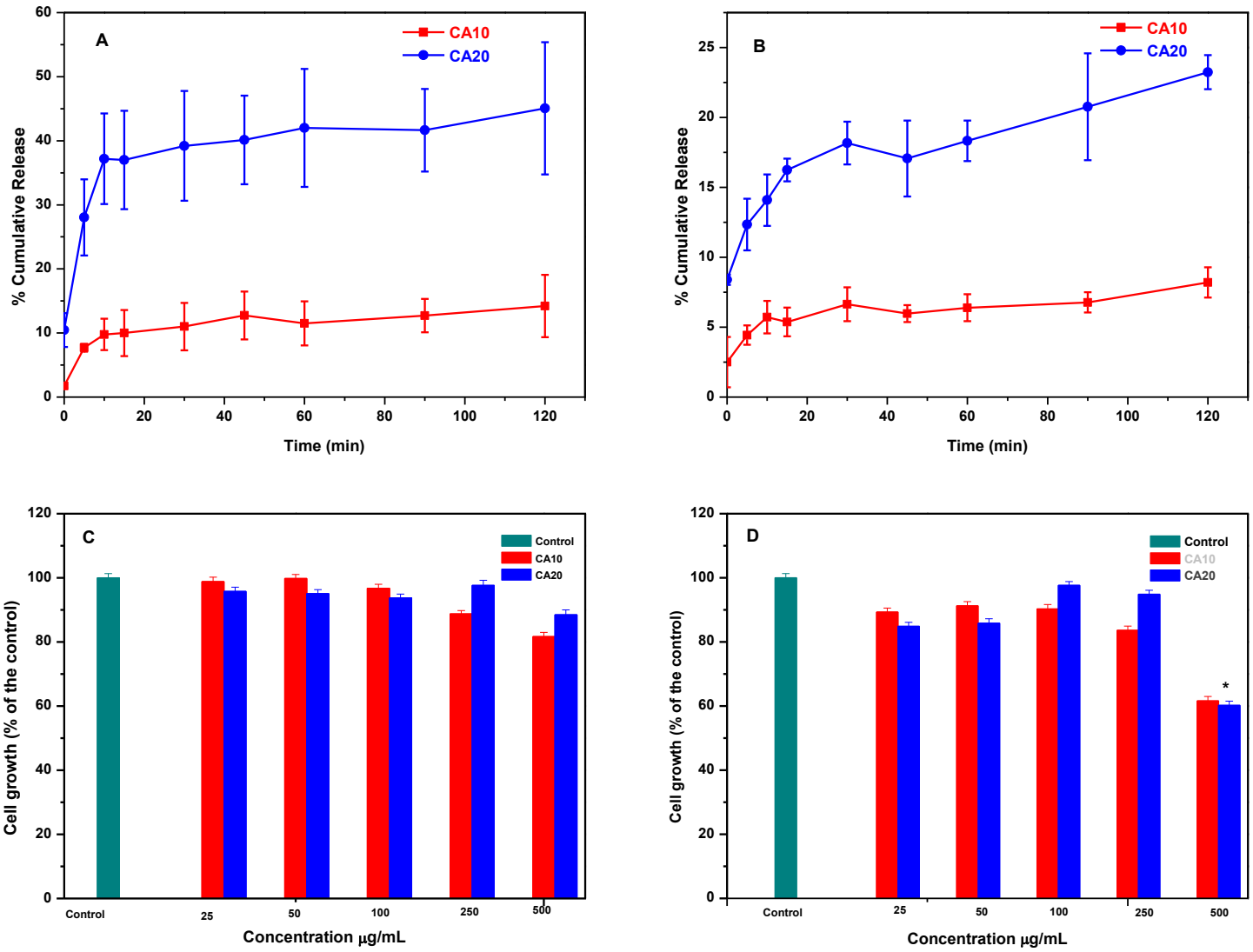

FIGURE 6

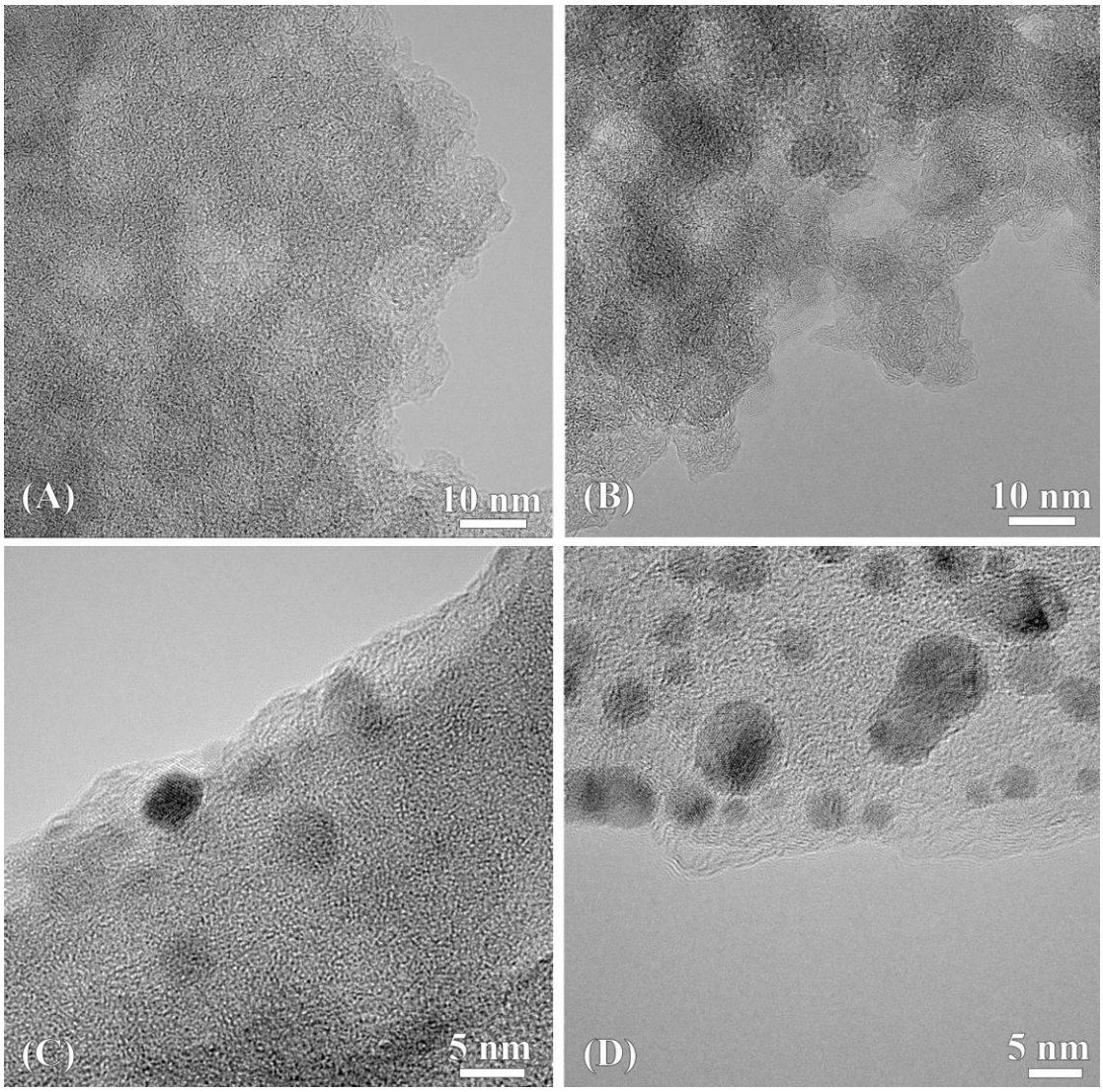

FIGURE 7

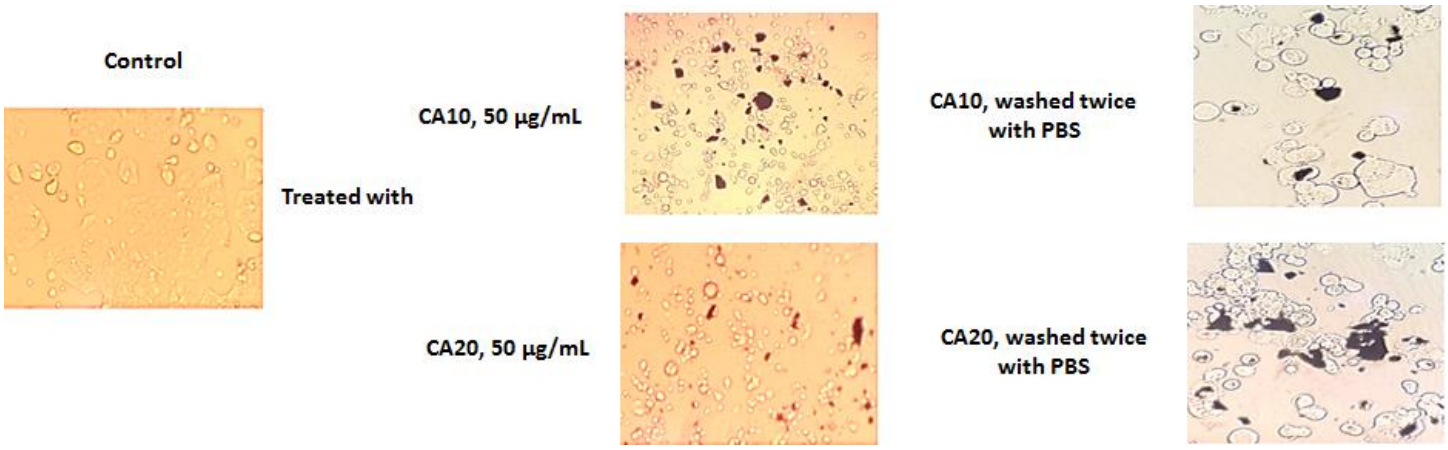

Table 1. Physicochemical characteristics of carbon aerogels. Mean pore size, BET specific surface area, total pore volume values, ζ-potential studies and surface atomic ratio O/C of the carbon aerogels CA10 and CA20 and their IBU loaded congeners.

	Mean pore size (nm)	S_{BET} (m^2/g)	Total Pore Volume (cm^3/g)	ζ-potential (mV)	O/C
IBU					0.15
CA10	8.0	756	0.78	-27.0 ± 0.55	0.20
CA20	13.5	757	1.36	-41.0 ± 3.55	0.22
CA10-IBU	7.9	343	0.61	-22.2 ± 0.76	0.19
CA20-IBU	12.7	314	1.03	-10.7 ± 2.68	0.14